ASTRONOMY & ASTROPHYSICS
SUPPLEMENT SERIES

JUNE I **1997**, PAGE 219

Astron. Astrophys. Suppl. Ser. **123,** 219-239 (1997)

The B3-VLA quasar sample⋆

M. Vigotti[1], G. Vettolani[1], R. Merighi[2], J.F. Lahulla[3], and M. Pedani[1]

[1] Istituto di Radioastronomia del CNR, Bologna, Italy
[2] Osservatorio Astronomico di Bologna, Italy
[3] Observatorio Astronomico de Madrid (O.A.N.-I.G.N.) Spain

Received July 22; accepted September 23, 1996

Abstract. A new low frequency radio selected Sample of 125 Quasars complete down to 100 mJy at 408 MHz is presented in this paper. The sample is a part of the B3-VLA sample: 1050 radiosources selected from the B3 catalogue at 408 MHz and observed at the VLA (1465 MHz, C and A configurations). Out of the 352 sources, identified on the POSS-I down to $m_r \sim 20.0$, 172 are quasar candidates. In this paper we give the final assessment of the quasar sample from spectroscopic observations of the candidates. The final complete quasar sample consists of 125 objects. Furthermore 3 Bl Lac objects have been identified and two Bl Lac candidates.

Key words: galaxies: active — quasars: general — radio continuum: general

1. Introduction

Quasars were first discovered through the optical identification of radio sources. Optical searches, based on different criteria from multicolor selection to grism searches, have produced a large number of optically selected quasar and have shown that radio loud quasars are really a fraction of the quasar population. However, optical multicolor searches have their own problems in completeness if, for instance, a large fraction of obscured quasars exists (Webster et al. 1995). In principle radio quasars samples do not suffer from a bias of this kind and, therefore, studying their color distribution, they should provide a direct test on the number of obscured quasars.

In the last years, a renewed interest is also raising in radio samples selected at low frequency because they provide an effective way to test the Unified Schemes (US) for extragalactic radiosources (Barthel 1989) through, for instance, a direct comparison of the observed angular sizes of radiogalaxies and quasars in the same redshift range.

Quasar samples selected at meter-wavelength are preferable with respect to high frequency selected samples because the source selection is largely based on their lobe emission. On the contrary flat spectrum sources, predominant in high frequency selected samples, are mostly core-dominated cases where the relativistic beaming might introduce serious selection effects.

Although US are generally accepted, some authors found observational evidences which cannot be explained by this scheme and that require a more complex treatment of the AGN phenomenon. Using 3CR, MQS, 1JY samples and an earlier version of the present B3−VLA quasar sample (see Singal 1993 and references therein), Singal finds several discrepancies between the predictions of US and the observational data. For instance, the observed number of quasars versus total source number, namely the quasar fraction (f_q) changes with the limiting flux of the sample. In the MQS sample, Kapahi et al. (1996) show that apparent sizes of radiogalaxies and quasars have almost an equal distribution at any redshift in contradiction with the US prediction. A similar result has been found by Blundell et al. (1996), using 3CR, 5C, 6C and 8C samples.

In a future paper, using all the available parameters of radiogalaxies and quasars of the B3−VLA sample (apparent diameters, flux, power, redshifts), we will verify the predictions of the US.

In Sect. 2 we present the final QSO sample based on spectroscopic observations reported in Vigotti et al. (1990), Lahulla et al. (1991) and further observations of the remaining candidates described in Sect. 3 of the present paper. Section 4 contains comments on some individual sources, and finally Sect. 5 summarizes the present data.

Send offprint requests to: M. Vigotti

⋆ Tables 4, 5, 6 and Figs. 1, 2, 3, 4, 6 are also available in electronic form at the CDS via anonymous ftp to: cdsarc.u-strasbg.fr (130.79.128.5) or via http://cdsweb.u-strasbg.fr/Abstract.html

2. The B3-VLA quasar sample

2.1. The radio sample

The B3 radiosource catalogue (Ficarra et al. 1985), lists 13354 sources brighter than 100 mJy at 408 MHz and covers 0.78 steradians in a sky strip from 37° to 47°, all hour angles.

From the B3, down to the catalogue limit of 0.1 Jy, Vigotti et al. (1989) selected five complete subsamples separated by equal increments in logarithmic flux density and containing approximately the same number of sources, through the choice of different declination limits for each subsample. Furthermore, the right ascention range was restricted to exclude sky areas at low galactic latitude (R.A. $23^{\rm h}00^{\rm m} - 03^{\rm h}00^{\rm m}$ and $07^{\rm h}00^{\rm m} - 15^{\rm h}00^{\rm m}$).

From VLA maps in C configuration at 1465 MHz for the 1103 sources in the sample, Vigotti et al. (1989) obtained radio positions (accurate to 0.5 arcsec rms) which allowed the optical identification on POSS-I prints based on positional coincidence. The analysis of these maps has also led to the exclusion of 53 sources from the sample because they were either lobes or because some sources joined to form a single source.

These sources were reobserved at the same frequency with the VLA in A configuration allowing a better resolution, i.e. HPBW 1.4 arcsec to be compared with 14 arcsecs of C configuration. A−configuration VLA maps will be presented elsewhere (Vigotti et al. 1996, in preparation).

The final radio sample contains 1050 radiosources. Table 1 shows the sample definitions, the number of sources and the solid angle covered in each subsample. All the sky area limits are at 1950.0 epoch, except the declination limits for sample 4, which correspond to the whole B3 catalogue, and are referred to 1978.0 epoch. The solid angles are corrected for the incompleteness regions of the B3 survey.

2.2. Identifications

Out of the original 352 identified objects, described in Vigotti et al. (1989), 183 were quasars candidates, defining a quasar candidate on the basis of its star-like appearance, regardless of the color, to avoid color biases.

These were examined using the positional coincidence between the optical and radio positions and the structural informations coming both from the A-configuration and C-configuration VLA maps. In order to build a complete sample of quasar candidates, we have accepted also identifications which are formally at low probability. For the unresolved sources the radio-optical rms displacement is $\sim 0\farcs75$ and the 3σ radius is $\sim 2\farcs5$, but we decided to extend the search up to $6''$. Infact, examining the radio-optical displacement histogram (see Fig. 1) for the 57 unresolved (in C-configuration) spectroscopically confirmed quasars, we see that the 3σ choice would have implied a loss of $\sim 7\%$ of the unresolved sources (4/57) with a displacement greater than $2\farcs5$. A posteriori looking the A-configuration maps we understand why the distribution is not gaussian. In all the four cases the quasar was coincident with the faint component of a double radiosource of $4-5$ arcseconds diameter, and with a very high flux ratio between the two radio components.

Furthermore, we obtained CCD images with the 1.5 meters Loiano Telescope of Bologna Observatory or with 3.5 meters telescope at Calar Alto of all the identified objects with uncertain optical classification from plates in the original sample, in order to be sure not to have missed any star-like object.

From the 183 quasar candidates in Vigotti et al. (1989) we excluded: (a) five candidates with $m_{\rm r} \geq 20.0m$ (0019+391, 0800+399, 0800+472, 0805+406 and 1357+392). (b) three candidates which from the A−configuration VLA maps turned into empty fields (0209+390, 1012+389 and 1317+389). (c) three candidates which revealed to be plate−flaws from CCD images (1033+408, 1258+395 and 1301+393).

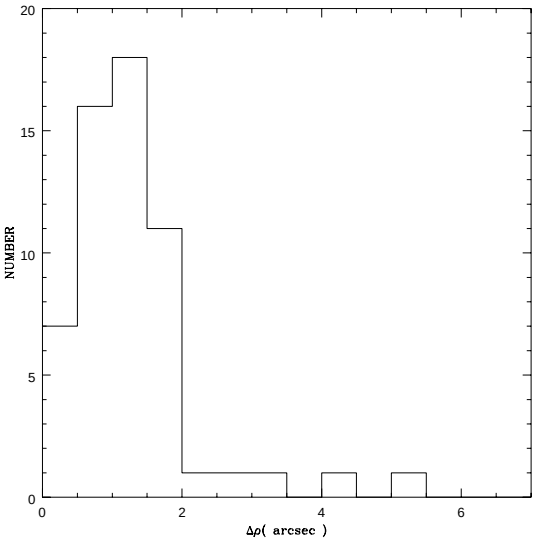

Fig. 1. Distribution of the radio–optical displacements for 57 unresolved quasars

2.3. Magnitudes

The candidates magnitudes in Vigotti et al. (1989) were estimates on POSS−I enlargements obtained by comparison with reference star images in the Selected Area 57. The accuracy of those estimated R magnitudes is 0.5 m. As machine measured R magnitudes are available from the APM Catalogue (Irwin 1992) which have an rms error of $\sim 0.3m$, we list these in Table 4. There is a good agreement between the two magnitude scales (see Fig. 2) with a $0.024m$ zero point. In two cases (0143+446b, 1342+389a) we adopted the estimated magnitudes because APM was

Table 1. Definition of the B3-VLA sample

Sample♯	Declination range	Flux−Density range (Jy)	Number of sources	Area Steradians
0	$+39°38'$ to $+40°00'$	$0.1 \leq S < 0.2$	168	0.0125
1	$+38°50'$ to $+40°00'$	$0.2 \leq S < 0.4$	256	0.0405
2	$+38°00'$ to $+40°48'$	$0.4 \leq S < 0.8$	252	0.0971
3	$+38°00'$ to $+44°30'$	$0.8 \leq S < 1.6$	208	0.2341
4	$+37°15'$ to $+47°37'$	$1.6 \leq S$	166	0.3813

clearly wrong (they were giving the magnitude of the quasar plus a star few seconds apart). The sample is complete down to POSS−I limit in red, nominally 20.0; however a plate to plate variation of 0.25 magnitudes could affect the sample.

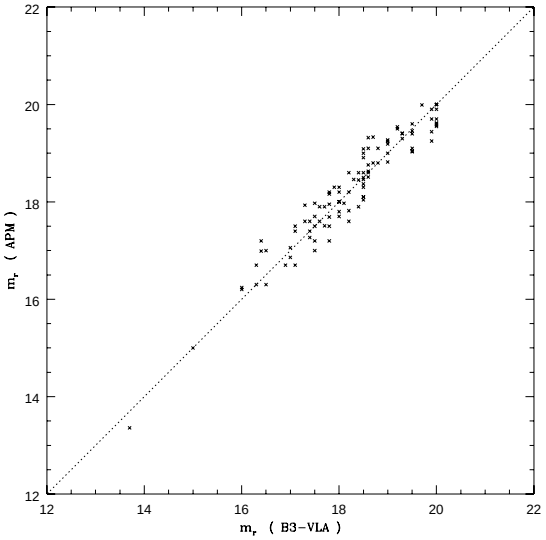

Fig. 2. B3 magnitudes versus APM magnitudes

3. The sample completeness

We can estimate the optical completeness of the sample, namely how many quasars are not included in our sample because their magnitude is fainter than 20.0 in red, as follows. In the sample with $S_{408} \geq 0.8$ Jy we can obtain a direct information: 55 EF out of 210 have been observed spectroscopically and only 1 EF turned out to be a quasar while all the other EF are high z radiogalaxies (Djorgovski private communication 1996). We therefore estimate that about 4 quasars are fainter than the POSS−I limit. There will be 68 Quasars in this radio flux bin, regardless of the optical magnitude limit, 64 brigther than 20 magnitudes and 4 hidden among the Empty Fields. This is in good agreement with another direct information obtained by Grueff & Vigotti (1975) by observing 113 Quasar candidates, at limiting flux of 0.9 Jy at 408 MHz, ($\sim$ 50% spectroscopically confirmed) down to $m_v = 22.5$. They found only 4% of the quasar sample fainter than POSS−I limit. However the question of how many quasars are in the EF has different answers depending from the flux limit and from the frequency selection of the sample. The magnitude histograms in Fig. 3 show that for samples selected at low frequency the sample incompleteness is negligible at higher flux (3CR or B3−VLA at $S \geq 0.8$ Jy). It is also evident that the median magnitude of the sample is becoming fainter in fainter flux bins. On the other hand lower flux samples c and d, as defined in Fig. 3, show a clear cut in the right side of the histogram due to the POSS−I magnitude limit. An approximate evaluation of the number of the quasars in EF versus the sample flux can be obtained af follows. As hinted from Fig. 3 we can assume that the shape of the magnitudes distribution in different flux bins does not vary with flux but the whole histogram is shifted towards fainter magnitudes at lower fluxes. We compute $D_{\rm med}$: the difference of the median magnitude of b and c samples in Fig. 3, we shift the magnitude distribution of sample b by $D_{\rm med}$ toward fainter magnitudes and finally we assume that the fraction of quasars that are in EF in the sample c is the same as for the new sample b. Than we recalculate the median of the sample c and repeat the procedure. This allows to have a reasonable estimate of the number of quasars hidden in EF for different flux intervals (see Table 2).

3.1. The final sample

The final sample now contains 172 quasar candidates brighter than $m_{\rm r} \leq 20.0$. The quasar candidates sample is further subdivided into 120 blue starlike objects (B) and 52 neutral color or red starlike objects (N).

For all the candidates (except 35 with literature redshifts available) spectra were obtained at the 2.2 m and 3.5 m telescopes of Calar Alto during various observing runs. Some earlier data from these observations are described in Vigotti et al. (1990), and Lahulla et al. (1991). The remaining data are described in Sect. 3.

Table 3 presents the final assessment of the B3-VLA quasar candidates identifications after the identification revision and the spectroscopic observations.

The relatively high number of misidentifications with stars is due to acceptance of low-probability Identifications

Table 2. Estimate of Quasars in EF

Flux Bin	Mean Flux (Jy)	# Quasars with $m_r \leq 20.0$	Quasars in EF	Median Mag.	Quasar Percentage in EF
$0.1 \div 0.4$	0.22	30	13	19.6	30
$0.4 \div 0.8$	0.53	31	12	19.3	28
≥ 0.8	2.25	64	4	18.2	6

Table 3. Identifications of the B3−VLA Quasar candidates sample

COLOR	CANDIDATES	QUASARS	GALAXIES	BL-LACs	STARS	FEATURELESS
B	120	110	0	2	5	3
N	52	15	22	1	13	1
TOTAL	172	125	22	3	18	4

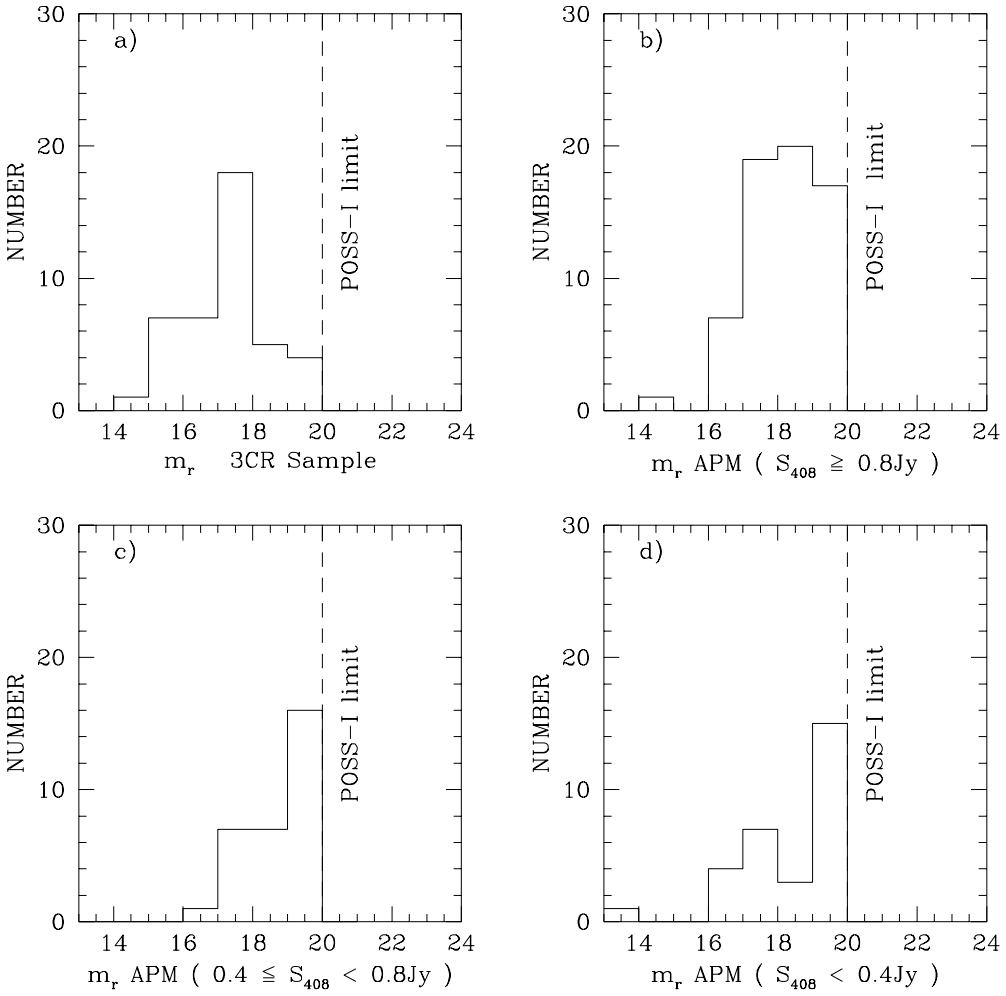

Fig. 3. The magnitudes distributions for different B3−VLA flux intervals and the 3CR sample. **a)** 3CR; **b)** $S_{408} \geq 0.8$ Jy; **c)** 0.4 Jy $\leq S_{408} < 0.8$ Jy; **d)** 0.1 Jy $\leq S_{408} < 0.4$ Jy

as described in Sect. 2.2. The 3 sources classified as BL Lac in Table 3 were previously known in literature. Four spectra are classified as featurless: two are possible BL-Lac candidates on the basis of their radio morphology: 2322+396 and 2311+396a. The former is unresolved (diam $\leq 0.5''$) and has flat radio spectral index (0.0) , while the latter is a less probable candidate, radio extended, diffuse and with a spectral index = -0.9. The remaining two objects with featureless spectra could be either galaxies or stars as they lack the typical radio characteristics of Bl-Lacs.

The final complete sample of quasars is presented in Table 4. Redshifts are available for 123 of the 125 spectroscopically confirmed quasar. The columns contain the following data: *Column 1:* name; *Column 2:* Right Ascention (1950.0) of the optical position (0.6 arcsec rms). *Column 3:* Declination (1950.0) of the optical position (0.6 arcsec rms). *Column 4:* Radio flux at 408 MHz. *Column 5:* APM red Magnitude. *Column 6:* Spectral Index. *Column 7:* Redshift. *Column 8:* Reference to published redshifts.

4. Observations of the quasar candidates

The observations of the quasar candidates candidates were accomplished with the Focal Reducer (Lenzen 1989) at the prime focus of the 3.5 meters telescope of the German-Spanish Astronomical Center at Calar Alto (Spain) during six observing runs: October 1989, March 1990, October 1990, February 1991, September 1991 and November 1992.

Our spectra cover a wavelength range from about 4000 to 9000 Å with resolution ~ 12 Å per pixel (except for the three last runs, when the focal reducer optics have been slightly modified giving a resolution of ~ 16 Å per pixel).

When the low dispersion spectrum showed no evident broad emission lines typical of quasars, the objects, with a few exceptions, were reobserved at higher dispersion (with a resolution of ~ 4 Å per pixel).

Flux calibration was obtained observing the following standard stars: Feige 98, Feige 15, Eggen 247 and HD 192281. Wavelength calibration spectra were obtained pointing to a screen in the dome illuminated by an He−Ar lamp. We decided to take only one series of He−Ar spectra at the end of each night, instead of one after each object, because of the conspicuous flexures arising from aiming at the screen near the dome floor. These flexures give rise to a wavelength shift which we corrected taking the NaI 5577 Å sky line as a reference zero−point. Furthermore, at low resolution the paucity and the poor definition of some lines of the He−Ar comparison spectrum near 4000 Å, has not allowed to obtain a good wavelength calibration in the blue region. In some cases the redshifts corresponding to the lines lying in the blue have been excluded in the calculation of the mean z.

Some representative spectra are shown in Fig. 4.

Table 5 lists the data for 77 of the 93 objects observed. The remaining 16 objects were spectroscopic stars and are listed in Table 6 together with other objects which changed the original identification, becoming "Empty Field" or "Galaxy".

The columns contain the following data: *Column 1:* name; *Column 2:* previous identification: *B* blue object, *N* red starlike object; *Column 3:* line identification; *Column 4:* observed wavelength; *Column 5:* rest wavelength adopted; *Column 6:* redshift computed for that line; *Column 7:* average redshift and eventually new spectroscopic identification, if not confirmed as Quasar.

To ease further studies of these objects, expecially of the few unsolved cases, we provide in Fig. 5 the finding charts for all the objects listed in the Table 5 and also for 8 objects listed in Table 6 identified as stars.

Table 6 lists objects whose identification changes due to spectroscopic and/or CCD observations. This table is intended to supplement table in Vigotti et al. (1989), where the optical coordinates are quoted.

5. Comments on individual sources

In this section some comments are collected for sources having peculiar or not well defined features in their spectra as well as details on a few objects whose identification changed from the original radio source identification.

0028+450: Our spectrum shows MgI (5175 Å) and NaI (5892 Å) at rest, thus we have classified this object as a star (see Table 6). However the identification is uncertain because Thomson et al. (1992) report the presence of one emission line which they identify as [OIII] (4983 Å at rest), thus classifying the object as a NELRG at $z = 0.365$.

0143+446b: The original identification was 14 magnitude red stellar object. In a CCD we discovered a fainter object about 4 arcsec south which revealed to be the true identification, i.e. a quasar with $m_r \sim 19$ (see Table 4).

0219+443: The spectrum only shows MgII, indicating a redshift of 0.852, in good agreement with Djorgovski et al. (1990) who find 0.850 from a spectrum with five lines (see Table 5).

0226+467: Only one broad line at about 6200 Å is present in our spectrum. We do not give the value of the redshift because of the poor Signal to Noise Ratio of the spectrum. If we identify the line as an MgII the redshift is ~ 1.216 (see Table 5).

0255+460: As mentioned earlier, our wavelength calibration has some uncertainties in the blue region of the spectrum. The feature at about 4240$\mathring{A}$ was identified as CIII, confirming the MgII at 6185 Å. The redshift reported in Table 5 is based on MgII only.

0724+396: The identification was with a galaxy of 16.5 mag which revealed to be a star. The Quasar is 5″SW and closer to radio centroid (see Table 4).

0809+404: We report spectral data for this object, though it was not included in the 172 quasar candidates

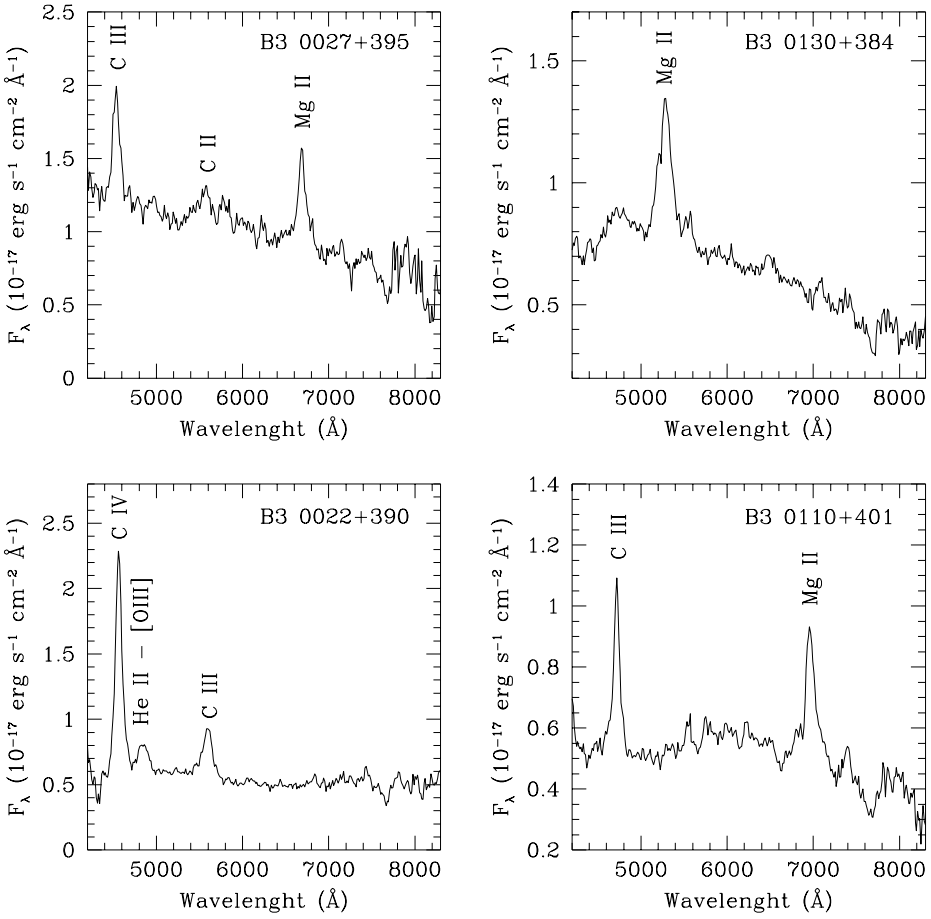

Fig. 4. Some representative spectra for the Quasars in the B3−VLA sample

sample. The original ID was G?, but it had stellar appearance on the CCD image. The spectrum classified it as Emission line Galaxy.

0912+392: The optical counterpart has been found 1.5 m fainter during the March 1990 observing run with respect to POSS−I.

0953+398: A broad line at about 4300 Å has been identified as CIII, confirming that a line at 6099 Å is MgII. The redshift derived from the CIII is not reported and the final value has been computed using MgII only (see Table 5).

1128+385: A line at about 4350 Å has been identified as CIV, confirming the feature at 5221 Å being CIII. The redshift relative to CIV is not reported because of problems with wavelength calibration at the blue end of the spectrum. The redshift is computed using CIII only (see Table 5).

1241+411: We report spectral data for this object, though it was not included in the 172 quasar candidates sample. The original ID was G?, but it had stellar appearance on the CCD image. The spectrum classified it as Emission line galaxy.

1416+400: A feature at about 4150 Å has been identified with MgII but we didn't use it for the redshift calculation because of problems with wavelength calibration in that region of the spectrum. The other lines present in the spectrum give anyway a good z measurement (see Table 5).

2316+398: The line at 7835 Å, identified as MgII, has a poor definition and it was not possible to obtain a secure value of the central wavelength, so we decided not to use it for the redshift determination. Thus the redshift has been computed using CIV only.

2322+396: The spectrum appears featureless but this may be due to the bad S/N ratio (see Table 5 and Table 6), thus the identification is uncertain.

2329+398: The spectrum shows only one emission line at about 5010 Å and wide enough to say that this is a Quasar. Since it was not possible to give a certain identification, the redshift is not reported.

6. Discussion

Out of 172 quasar candidates we have obtained a complete sample of 125 quasars. Figure 6 show the redshift

distribution for the 123 quasars whose z is known. The median redshift (dashed line) is 1.16. Of the remaining candidates 1 is a Seyfert galaxy, 5 are narrow emission line galaxies, 17 are normal galaxies, 17 have been reclassified as empty fields as the proposed identification turned out being a galactic star, 4 objects have featureless spectra so they can be Galaxies or Stars or Bl− Lacs.

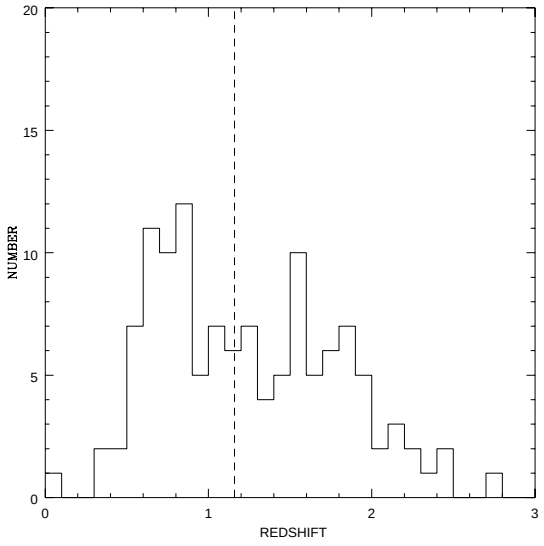

Fig. 6. Redshift distribution for the Quasars in the B3−VLA sample. The dashed vertical line indicates the median redshift: $z = 1.16$

Acknowledgements. We would like to thank the German-Spanish Astronomical Center, operated by the Max Plank Institute für Astronomie (Heidelberg), jointly with the Spanish National Commission for Astronomy.

References

Allington-Smith J.R., Spinrad H., Djorgowski S., Liebert J., 1988, MNRAS 234, 1091
Arp H., De Ruiter H.R., Willis A.G., 1979, A&A 77, 86
Baldwin J.A, Burbidge E.M., Hazard C., Murdoch H.S., Robinson L.B., Wampler E.J., 1973, ApJ 185, 739
Barthel P.D., 1989, ApJ 336, 606
Blundell K.M., Rawlings S., Eales S.A., Lacy M., 1996, New results from complete samples of faint radio Galaxies and Quasars. In: Erkes R., Fanti C., Padrielli L. (eds.) Proc. IAU Symp. 175, Extra galactic radio sources. Kluwer, Dordrecht (in press)
Burbidge E.M., Kinman T.D., 1966, ApJ 145, 654
Burbidge E.M., 1968, ApJ 154, L109
Burbidge E.M., Strittmatter P.A., 1972, ApJ 174, L57
Djorgovski S., Thomson D.J., Vigotti M., Grueff G., 1990, PASP 102, 113
Djorgovski S., Thomson D., Maxfield L., Vigotti M., Grueff G., 1995, ApJS 101, 255
Ficarra A., Grueff G., Tomassetti G., 1985, A&AS 59, 255
Grueff G., Vigotti M., 1975, A&AS 20, 57
Hiltner W.A., Cowley A.P., Schild R.E., 1966, PASP 78, 464
Kapahi V.K., Athreya R.M., Subrahmanya C.R., et al., 1996, Radio structures of the MRC 1-Jy sources and the unification of radio Galaxies and Quasars. In: Erkes R., Fanti C., Padrielli L. (eds.), Proc. IAU Symp. 175, Extra galactic radio sources. Kluwer, Dordrecht (in press)
Kühr H., Schmidt G.D., 1990, AJ 99, 1
Irwin M., 1992, Gemini 37, 1 Newsletter of the Royal Greenwich Observatory
Lahulla J.F., Merighi R., Vettolani G., Vigotti M., 1991, A&AS 88, 525
Lenzen R., 1989, Focal Reducer for the prime focus of the 3.5 m Telescope, MPI fur Astronomie, Heidelberg
Lynds C.R., 1967, ApJ 147, 837
Owen F.N., Porcas R.W., Neff S.G., 1978, AJ 83, 1009
Schmidt M., 1965, ApJ 141, 1295
Schmidt M., 1974, ApJ 193, 505
Schmidt M., 1968, ApJ 151, 393
Singal A.K., 1993, MNRAS 263, 139
Smith H.E., Spinrad H., 1980, ApJ 236, 419
Steidel C.C., Sargent W.L.W., 1991, ApJ 382, 433
St:89 Stephens S.A., 1989, AJ 97, 10
Stickel M., Khur H., 1993, A&AS 101, 521
Stickel M., Khur H., 1994, A&AS 103, 349
Thomson D.J., Djorgovski S., Vigotti M., Grueff G., 1992, ApJS 81, 1
Tytler D., Fan X.M., 1992, ApJS 79, 1
Veron-Cetty M.P., Veron P., 1993, ESO scientific report 13
Vigotti M., Grueff G., Perley R., Clark B.G., Bridle A.H., 1989, AJ 98, 419
Vigotti M., Merighi R., Vettolani G., Lahulla J.F., Lopez-Arroyo M., 1990, A&AS 83, 205
Walsh D., Carswell R.F., 1982, MNRAS 200, 191
Walsh D., Beckers J.M., Carswell R.F., Weymann R.J., 1984, MNRAS 211, 105
Walsh D., Wills B.J., Wills D., 1979, MNRAS 189, 667
Webster R.L., Francis P.J., Peterson B.A., Drinkwater M.J., Masci F.J., 1995, Nat 375, 469
Wills B.J., Browne I.W.A., 1986, ApJ 302, 56
Wills D., Wills B.J., 1976, ApJS 31, 143
Wills D., Wills B.J., 1985, (private communication)
Xu W., Lawrence C.R., Readhead A.C.S., Pearson T.J., 1994, AJ 108, 395

Table 4. The B3-VLA Quasars complete sample

B3 name	R.A.(B 1950.0)	Dec.	S 408 MHz (Jy)	Sp.Ind.	m_r	z	ref.
			Sample 0 : $0.1 \leq S < 0.2$ Jy				
0107+398	01 07 54.05	+39 51 22.2	0.11	0.90	18.8	0.823	
0158+394	01 59 00.20	+39 28 55.0	0.12	0.18	18.4	0.780	
0209+394	02 09 33.86	+39 28 16.3	0.13	0.50	19.1	0.927	
0739+398	07 39 13.28	+39 51 42.4	0.17	0.22	19.4	2.186	
0754+394	07 54 38.20	+39 28 34.0	0.13	1.03	13.4	0.096	Stephens 89
1019+397	10 19 40.57	+39 47 00.8	0.17	0.86	16.2	0.605	Vigotti 90
1251+398	12 51 49.36	+39 49 38.6	0.15	0.93	19.5	2.104	Lahulla 91
1259+395	12 59 41.76	+39 31 32.0	0.10	1.05	19.5	0.577	
1338+394	13 38 57.59	+39 29 57.4	0.18	0.68	19.2	0.580	Lahulla 91
1356+397	13 56 08.84	+39 47 16.8	0.12	0.73	19.6	0.594	
1419+399	14 19 23.92	+39 57 08.0	0.14	0.44	17.6	0.622	Vigotti 90
2329+398	23 29 46.68	+39 50 43.8	0.18	1.12	20.0	?	
			Sample 1 : $0.2 \leq S < 0.4$ Jy				
0022+399	00 22 03.51	+39 59 36.4	0.20	0.58	20.0	1.983	
0034+393	00 34 54.24	+39 21 42.4	0.20	−.08	17.0	1.937	Baldwin 73
0207+395	02 07 07.47	+39 35 51.6	0.36	0.96	18.0	0.818	
0225+389	02 25 52.93	+38 54 22.5	0.22	0.70	16.4	0.336	Djorgovski 95
0239+397	02 39 44.63	+39 43 00.7	0.37	0.86	20.0	1.159	
0724+396	07 24 45.10	+39 36 38.0	0.24	1.09	19.8	2.753	
0729+391	07 29 57.02	+39 11 34.9	0.26	0.43	17.9	0.663	Djorgovski 90
0824+397	08 24 48.59	+39 45 38.5	0.27	0.95	17.5	0.760	Vigotti 90
0912+392	09 12 55.43	+39 12 50.9	0.21	1.08	20.0	1.978	
0935+397	09 35 33.06	+39 47 52.5	0.32	0.63	19.1	2.493	
1116+392	11 16 19.50	+39 15 17.5	0.36	0.91	17.7	0.733	Vigotti 90
1123+395	11 23 45.85	+39 35 15.1	0.36	0.82	17.0	1.470	Vigotti 90
1204+399	12 04 04.55	+39 57 44.8	0.34	0.39	17.6	1.530	Wills 85
1212+389	12 12 43.28	+38 56 02.8	0.30	1.01	20.0	2.356	
1300+397	13 00 29.06	+39 46 07.6	0.27	0.89	18.2	2.436	Vigotti 90
1349+388	13 49 10.63	+38 53 03.4	0.22	−.05	20.0	1.888	
2316+398	23 16 57.66	+39 53 38.5	0.29	0.93	20.0	1.846	
			Sample 2 : $0.4 \leq S < 0.8$ Jy				
0013+387	00 13 22.79	+38 43 47.0	0.74	0.98	18.5	1.721	
0027+380	00 27 42.10	+38 00 47.2	0.58	1.08	19.3	1.066	
0027+395	00 27 03.23	+39 32 03.4	0.41	0.69	18.5	1.388	
0106+380	01 06 36.49	+38 00 47.8	0.45	0.74	16.9	0.583	Wills 86
0130+384	01 30 05.06	+38 25 38.1	0.53	1.01	19.3	0.889	
0139+389A	01 39 13.02	+38 57 34.4	0.43	0.67	20.0	1.106	
0756+406	07 56 52.69	+40 38 10.6	0.50	0.86	18.8	2.016	
0802+398	08 02 36.62	+39 49 22.4	0.41	1.01	19.6	1.800	
0904+386	09 04 35.15	+38 39 46.5	0.43	0.83	17.7	1.730	Wills 85
0907+381	09 07 44.92	+38 11 32.5	0.43	0.39	17.3	2.160	Wills 85
0910+392	09 10 42.31	+39 14 37.7	0.41	1.08	19.2	0.638	Lahulla 91
0922+407	09 22 50.59	+40 42 48.6	0.48	0.33	19.6	1.876	
0926+388	09 26 34.45	+38 49 13.6	0.50	1.09	18.3	1.630	Lahulla 91
0953+398	09 53 05.90	+39 49 32.1	0.50	0.41	19.7	1.179	
1015+383	10 15 28.92	+38 20 34.5	0.64	0.86	17.7	0.380	Wills 85
1128+385	11 28 12.55	+38 31 52.3	0.52	−.33	18.6	1.735	Xu 94

Table 4. continued

B3 name	R.A. (B 1950.0)	Dec.	S 408 MHz (Jy)	Sp.Ind.	m_r	z	ref.
1141+400	11 41 55.26	+40 00 02.2	0.41	0.95	18.5	0.907	
1142+392	11 42 56.29	+39 13 26.0	0.57	1.02	18.0	2.276	
1203+384	12 03 44.74	+38 29 17.3	0.67	0.98	18.0	0.838	Vigotti 90
1228+397	12 28 25.90	+39 46 33.8	0.60	0.89	17.9	2.217	Vigotti 90
1240+381	12 40 27.03	+38 07 25.1	0.41	−.02	19.1	1.316	
1312+393	13 12 49.52	+39 19 31.7	0.71	0.95	20.0	1.570	
1317+380	13 17 36.20	+38 03 08.4	0.75	0.86	19.1	0.835	Lahulla 91
1348+392	13 48 23.61	+39 14 12.6	0.50	0.92	19.3	1.580	Lahulla 91
1355+380	13 55 30.54	+38 04 04.9	0.60	0.89	19.3	1.561	
1357+394B	13 57 56.50	+39 25 25.7	0.41	1.08	19.6	0.804	
1416+400	14 16 56.66	+40 00 24.8	0.67	0.96	20.0	0.473	
1417+385	14 17 43.05	+38 35 32.6	0.47	−.37	19.4	1.832	Lahulla 91
1435+383	14 35 33.32	+38 20 43.7	0.54	0.85	17.1	1.600	Vigotti 90
2327+407	23 27 42.88	+40 47 51.8	0.48	0.56	18.0	1.220	Vigotti 90
2335+392	23 35 43.32	+39 16 55.5	0.56	0.93	18.8	1.059	
2338+390	23 38 44.84	+39 01 49.3	0.62	0.98	20.0	0.816	
		Sample 3 : $0.8 \leq S < 1.6$ Jy					
0006+397	00 06 28.54	+39 45 05.2	1.15	0.66	19.5	1.830	Wills 85
0022+390	00 22 46.64	+39 02 58.9	1.10	0.10	18.6	1.932	
0032+423	00 32 23.26	+42 21 49.6	0.92	0.94	18.2	1.588	Burbidge 68
0110+401	01 10 26.48	+40 10 19.6	1.08	0.65	19.7	1.479	
0137+401	01 37 36.18	+40 09 03.9	0.82	0.85	18.9	1.62	
0144+430	01 44 55.86	+43 04 48.1	0.92	1.01	19.3	1.790	
0217+417	02 17 06.31	+41 43 56.9	0.85	0.94	18.4	1.430	Arp 79
0219+443	02 19 06.20	+44 19 17.8	0.89	1.17	17.9	0.852	Djorgovski 90
0224+393	02 24 00.97	+39 18 14.2	0.89	0.68	19.0	1.571	
0249+383	02 49 58.98	+38 23 10.9	0.95	0.34	18.5	1.12	
0701+392	07 01 05.07	+39 15 54.3	1.17	0.75	18.8	1.283	Lahulla 91
0726+431	07 26 16.70	+43 07 35.5	1.29	1.17	18.2	1.072	Wills 76
0739+397B	07 39 45.93	+39 48 39.8	1.02	0.57	18.0	1.700	Lahulla 91
0829+425	08 29 26.28	+42 35 12.5	0.82	0.56	18.6	1.056	
0836+426	08 36 35.50	+42 38 34.1	1.12	0.65	19.6	0.595	
0849+424	08 49 15.71	+42 26 47.5	1.31	0.90	18.0	0.978	Vigotti 90
0922+422	09 22 47.56	+42 16 37.2	0.97	1.20	18.3	1.750	Vigotti 90
0922+425	09 22 12.43	+42 30 28.3	1.15	1.22	19.4	1.879	
0951+408	09 51 39.03	+40 50 56.5	0.92	1.03	18.5	0.783	
0955+387	09 55 01.70	+38 44 19.3	1.42	1.10	20.0	1.405	Allington 88
1030+415	10 30 07.78	+41 31 34.0	1.02	0.43	17.4	1.120	Walsh 79
1144+402	11 44 20.98	+40 15 13.9	0.93	−.06	18.0	1.010	Stickel 94
1229+405	12 29 13.84	+40 34 02.4	0.91	0.98	19.0	0.649	Lahulla 91
1239+442B	12 39 57.00	+44 12 34.3	1.21	0.92	17.8	0.610	Vigotti 90
1256+392	12 56 41.87	+39 16 22.9	0.80	1.03	17.9	0.978	Vigotti 90
1315+396	13 15 02.86	+39 41 15.4	1.16	0.49	17.6	1.560	Vigotti 90
1341+392	13 41 10.09	+39 13 35.3	1.22	1.01	19.9	0.768	
1342+389A	13 42 15.11	+38 56 31.3	0.86	1.09	17.6	1.533	Lahulla 91
1343+386	13 43 26.76	+38 38 12.1	1.52	0.48	17.5	1.844	Schmidt 74
1444+417A	14 44 32.36	+41 45 50.1	1.58	1.03	17.8	0.675	Lahulla 91
2344+429	23 44 52.88	+42 54 12.7	0.92	0.58	18.3	1.556	
2349+410	23 49 21.46	+41 04 34.0	1.38	0.98	19.8	2.046	

Table 4. continued

B3 name	R.A. (B 1950.0)	Dec.	S 408 MHz (Jy)	Sp.Ind.	m_r	z	ref.
			Sample 4 : $S \geq 1.6$ Jy				
0019+431	00 19 08.17	+43 11 47.1	2.22	1.34	19.4	1.050	
0143+446B	01 43 45.30	+44 40 21.0	1.71	0.99	17.8	0.813	Thomson 92
0157+442	01 57 32.74	+44 12 44.6	3.26	0.91	19.2	0.721	
0226+467	02 26 05.20	+46 46 54.0	2.45	0.93	20.0	?	
0232+411B	02 32 45.82	+41 10 13.5	2.75	0.99	17.4	0.500	
0255+460	02 55 08.10	+46 04 06.0	1.74	0.77	20.0	1.21	
0704+384	07 04 08.41	+38 26 56.8	2.87	1.06	17.4	0.579	Schmidt 74
0740+380C	07 40 56.75	+38 00 31.6	5.55	1.29	16.7	1.063	Hiltner 66
0821+394	08 21 37.31	+39 26 27.7	2.59	0.58	17.5	1.216	Schmidt 74
0821+447	08 21 50.27	+44 46 14.2	2.26	0.90	17.0	0.893	Walsh 82
0827+378	08 27 55.10	+37 52 18.2	5.17	0.80	18.2	0.914	Lynds 67
0859+470	08 59 39.90	+47 02 57.0	2.81	0.21	18.6	1.462	Walsh 82
0906+430	09 06 17.26	+43 05 58.0	11.90	0.87	18.0	0.670	Smith 80
0913+391	09 13 39.50	+39 07 01.7	1.65	0.25	18.1	1.250	Stickel 94
0918+381	09 18 39.27	+38 06 57.7	2.45	1.07	19.1	1.108	Lahulla 91
0923+392	09 23 55.29	+39 15 23.4	3.33	0.09	16.9	0.698	Burbidge 66
0937+391	09 37 59.10	+39 07 31.0	1.88	0.86	17.5	0.618	Burbidge 72
0945+408	09 45 50.16	+40 53 44.1	2.45	0.51	17.2	1.252	Walsh 82
1007+417	10 07 26.13	+41 47 25.3	4.10	0.79	15.0	0.613	Owen 78
1020+400	10 20 14.56	+40 03 26.8	1.77	0.37	16.7	1.250	Xu 94
1105+392	11 05 51.57	+39 14 56.2	2.31	0.87	18.1	0.781	Lahulla 91
1109+437	11 09 52.28	+43 42 06.1	4.77	1.09	18.6	1.680	Walsh 84
1111+408	11 11 53.28	+40 53 41.9	10.92	1.16	16.3	0.734	Schmidt 65
1148+387	11 48 53.32	+38 42 34.4	1.83	0.94	16.2	1.303	Steidel 91
1148+477	11 48 32.28	+47 45 36.1	2.29	1.19	17.2	0.867	Walsh 84
1206+439B	12 06 42.06	+43 56 01.9	5.69	0.85	16.7	1.400	Schmidt 68
1242+410	12 42 26.37	+41 04 30.2	2.01	0.25	19.1	0.811	
1247+450A	12 47 03.61	+45 01 10.9	1.68	0.73	17.2	0.799	Walsh 84
1258+404	12 58 13.99	+40 25 15.9	4.51	1.04	19.0	1.656	Tytler 92
1339+472	13 39 41.72	+47 12 24.6	2.21	1.02	19.9	0.502	
2311+469	23 11 29.14	+46 55 54.5	4.34	0.69	18.1	0.745	
2351+456	23 51 50.04	+45 36 23.0	2.21	0.27	20.0	2.000	Stickel 93

Table 5. Lines identification and redshifts

B3 name	ID	Line	obs.	rest	z	average z, new ID
0003+380	N	[O II]	4581	3727	0.229	
		H ϵ	4752	3835	0.239	Seyfert
		H γ	5349	4340	0.232	$< z > = 0.234 \pm 0.005$
		H β	5976	4861	0.229	
		[O III]	6155	5007	0.235	
		H α	8140	6562	0.241	
0013+387	B	C IV	4215	1549	1.721	
		C III	5181	1909	1.714	$< z > = 1.721 \pm 0.007$
		C II	6345	2326	1.728	
0019+431	B	Mg II	5742	2798	1.052	
		[O III]	6419	3133	1.049	$< z > = 1.05 \pm 0.002$
0020+437	B	Featureless				Gal/Star
0022+390	B	C IV	4540	1549	1.931	
		HeII - [OIII]				
		blended	4847	1651	1.936	$< z > = 1.932 \pm 0.003$
		C III	5593	1909	1.930	
0022+399	B	C III	4621	1909	1.983	
		C IV	5696	1549	1.984	$< z > = 1.983 \pm 0.001$
0022+424	N	Mg I (abs.)	6215	5167	0.203	Galaxy
		Na (abs.)	7095	5892	0.204	$< z > = 0.203 \pm 0.001$
0023+382	N	Hθ (abs.)	5118	3798	0.347	
		Hδ (abs.)	5577	4101	0.359	Galaxy
		G band (abs.)	5849	4304	0.359	$< z > = 0.355 \pm 0.006$
		Mg I (abs.)	6998	5167	0.354	
0027+380	B	Mg II	5753	2798	1.056	
		[O II]	7738	3727	1.076	$< z > = 1.066 \pm 0.014$
0027+395	B	C III	4537	1909	1.377	
		C II	5575	2326	1.397	$< z > = 1.388 \pm 0.011$
		Mg II	6688	2798	1.383	
0035+385a	B	Featureless				Gal/Star
0045+395	N	Featureless				BL-Lac
0107+398	B	Mg II	5087	2798	0.818	
		[Ne V]	6260	3426	0.827	$< z > = 0.823 \pm 0.006$
0110+401	B	C III	4719	1909	1.472	
		Mg II	6958	2798	1.487	$< z > = 1.479 \pm 0.011$
0130+384	B	Mg II	5280	2798	0.887	
		[Ne V]	6479	3426	0.891	$< z > = 0.889 \pm 0.003$
0137+401	B	C III	4982	1909	1.61	
		Mg II	7360	2798	1.63	$< z > = 1.62 \pm 0.01$
0139+389a	B	Mg II	5895	2798	1.106	
		Ne IV	5105	2424	1.107	$< z > = 1.106 \pm 0.001$
0144+430	B	C IV	4327	1549	1.793	
		C III	5320	1909	1.787	$< z > = 1.79 \pm 0.004$
0153+417	N	[Ne V]	5090	3426	0.485	Em.lin.Gal.
		[O II]	5535	3727	0.485	$< z > = 0.488 \pm 0.005$
		[O III]	7477	5007	0.493	
0157+442	N	Mg II	4800	2798	0.716	
		[O II]	6397	3727	0.703	
		[Ne III]	6645	3870	0.717	
		H ϵ - Ne III				
		blended	6830	3968	0.721	$< z > = 0.721 \pm 0.008$
		H δ	7054	4101	0.720	
		H γ	7487	4340	0.725	
		[O III]	8643	5007	0.726	

Table 5. continued

B3 name	ID	Line	obs.	rest	z	average z, new ID
0158+394	B	Mg II	4977	2798	0.78	
0207+395	B	Mg II	5088	2798	0.818	
0209+394	B	Mg II	5392	2798	0.927	
0219+443	B	Mg II	5183	2798	0.852	
0224+393	B	C III	4904	1909	1.569	
		Mg II	7200	2798	1.573	$< z > = 1.571 \pm 0.003$
0225+389	B	[O III]				
		blend	6700	4983	0.344	
0226+467	N	?	≈6200			Quasar
0232+411b	B	Mg II	4195	2798	0.499	
		[Ne V]	5145	3426	0.502	
		[O II]	5598	3727	0.502	
		[Ne III]	5804	3870	0.500	
		H ϵ - Ne III				$< z > = 0.500 \pm 0.002$
		blended	5942	3968	0.497	
		H δ	6151	4101	0.500	
		H γ	6516	4340	0.501	
		[O III]	6546	4363	0.500	
0239+397	B	Mg II	6040	2798	1.159	
0249+383	B	Mg II	5930	2798	1.12	
0255+460	B	C III	≈4240	1909		
		Mg II	6185	2798	1.21	$z = 1.21$
0709+409	N					Galaxy from CCD image
0724+396	N	Ly α	4575	1216	2.762	
		O IV - Si IV				
		blended	5280	1405	2.758	$< z > = 2.753 \pm 0.013$
		C IV	5790	1549	2.738	
		C III	7120	1909	2.730	
0739+398	B	O IV - Si IV				
		blended	4476	1405	2.186	
		C IV	4932	1549	2.184	$< z > = 2.186 \pm 0.002$
		C III	6088	1909	2.189	
0756+406	B	C IV	4716	1549	2.044	
		C III	5724	1909	1.988	$< z > = 2.016 \pm 0.039$
0802+398	B	C IV	4339	1549	1.801	
		He II	4593	1640	1.801	$< z > = 1.800 \pm 0.002$
		C III	5339	1909	1.797	
		Mg II	7862	2798	1.801	
0809+404	G	[Ne V]	5585	3426	0.630	
		[O II]	5781	3727	0.551	
		[Ne III]	6000	3870	0.550	Seyfert
		H δ	6333	4101	0.544	$< z > = 0.551 \pm 0.003$
		H β	7552	4861	0.554	
		[O III]	7697	4959	0.552	
		[O III]	7773	5007	0.552	
0820+431	N					Galaxy from CCD image
0829+425	B	Mg II	5750	2798	1.055	
		[O III]	6443	3133	1.056	$< z > = 1.056 \pm 0.001$
0836+426	B	Mg II	4466	2798	0.596	
		[O II]	5929	3727	0.591	$< z > = 0.595 \pm 0.004$
		[O III]	6974	4363	0.598	
0841+403	N					Galaxy from CCD image
0902+414	N					Galaxy from CCD image
0904+399	N					Galaxy from CCD image

Table 5. continued

B3 name	ID	Line	obs.	rest	z	average z, new ID
0912+392	B	Ly α	3639	1216	1.993	
		C IV	4624	1549	1.985	$< z > = 1.978 \pm 0.019$
		C III	5643	1909	1.956	
0922+407	B	C IV	4448	1549	1.872	
		[O III]	4754	1663	1.859	$< z > = 1.876 \pm 0.01$
		C III	5478	1909	1.869	
		Mg II	8075	2798	1.886	
0922+425	N	C IV	4450	1549	1.873	
		C III	5510	1909	1.886	$< z > = 1.879 \pm 0.01$
0935+397	N	Ly α	4249	1216	2.494	
		O IV - Si IV				
		blended	4883	1405	2.488	$< z > = 2.493 \pm 0.003$
		C IV	5413	1549	2.494	
		C III	6674	1909	2.496	
0936+405	N	[O II]	4444	3727	0.192	
		[O III]	5899	5007	0.178	Em.lin.Gal.
		[O I]	7485	6300	0.188	$< z > = 0.186 \pm 0.005$
		H α	7779	6562	0.185	
		S II	7981	6731	0.186	
0951+408	B	Mg II	4989	2798	0.783	
		[Ne V]	6108	3426	0.783	$< z > = 0.783$
0953+398	N	C III	≈4300	1909		
		Mg II	6099	2798	1.179	
1128+385	B	C IV	≈4350	1549		
		C III	5221	1909	1.735	
1128+455	N	[O II]	5217	3727	0.409	Em.lin.Gal.
		[O III]				$< z > = 0.404 \pm 0.007$
		blend	7023	4983	0.400	
1141+400	N	Mg II	5336	2798	0.907	
1141+466	G	H β (abs.)	5261	4861	0.092	
		Mg I (abs.)	5680	5167	0.098	$< z > = 0.092 \pm 0.009$
		H α (abs.)	7206	6562	0.098	
1142+392	B	O IV - Si IV				
		blended	4604	1405	2.277	
		C IV	5075	1549	2.276	$< z > = 2.276 \pm 0.001$
		C III	6254	1909	2.276	
1212+389	B	O IV - Si IV				
		blended	4703	1405	2.347	
		C IV	5218	1549	2.369	
		HeII - [O III]				$< z > = 2.356 \pm 0.013$
		blended	5520	1651	2.342	
		C III	6427	1909	2.367	
1241+411	G	[O III]	3907	3133	0.247	
		[O III]				$< z > = 0.259 \pm 0.011$
		blend	6278	4983	0.260	AGN
		H α	8333	6562	0.269	
1242+410	B	Mg II	5052	2798	0.806	
		[O II]	6768	3727	0.816	$< z > = 0.811 \pm 0.007$
1259+395	B	Mg II	4412	2798	0.577	
1312+393	B	C III	4923	1909	1.579	
		Mg II	7160	2798	1.559	$< z > = 1.57 \pm 0.01$
1339+472	B	Mg II	≈4250	2798		
		[Ne V]	5128	3426	0.500	
		[O II]	5582	3727	0.501	
		[Ne III]	5797	3870	0.499	
		H ϵ - Ne III				$< z > = 0.502 \pm 0.003$

Table 5. continued

B3 name	ID	Line	obs.	rest	z	average z, new ID
		blended	5942	3968	0.497	
		H δ	6156	4101	0.501	
		H γ	6522	4340	0.503	
		H β	7332	4861	0.508	
		[O III]	7536	5007	0.505	
1341+392	N	Mg II	4945	2798	0.767	
		[Ne V]	6044	3426	0.764	
		[O II]	6595	3727	0.769	$< z > = 0.768 \pm 0.003$
		[Ne III]	6855	3870	0.772	
1349+388	B	C IV	4475	1549	1.889	
		C III	5510	1909	1.886	$< z > = 1.888 \pm 0.002$
1355+380	B	[O III]	4246	1663	1.553	
		C III	4880	1909	1.556	$< z > = 1.561 \pm 0.011$
		Mg II	7200	2798	1.574	
1356+397	B	Mg II	4438	2798	0.586	
		[Ne V]	5445	3426	0.589	
		[O II]	5945	3727	0.595	$< z > = 0.594 \pm 0.006$
		[Ne III]	6177	3870	0.596	
		H β	7781	4861	0.601	
		[O III]	8005	5007	0.599	
1357+394b	B	Mg II	5032	2798	0.798	
		[Ne V]	6188	3426	0.806	$< z > = 0.804 \pm 0.005$
		[O II]	6733	3727	0.806	
1416+400	B	Mg II	$\approx$4150	2798		
		[Ne V]	5045	3426	0.472	
		[O II]	5485	3727	0.472	
		[Ne III]	5701	3870	0.473	
		H ϵ - Ne III				
		blended	5836	3968	0.471	$< z > = 0.473 \pm 0.003$
		H δ	6037	4101	0.473	
		H γ	6410	4340	0.470	
		H β	7194	4861	0.479	
		[O III]	7410	5007	0.479	
1432+397b	N					Galaxy from CCD image
2311+396a	N	Featureless				Gal/Star/BL-Lac
2311+469	B	Mg II	4885	2798	0.746	
		He II	5596	3203	0.747	
		[Ne V]	5973	3426	0.743	$< z > = 0.745 \pm 0.002$
		[Ne III]	6744	3870	0.743	
2316+398	B	C IV	4409	1549	1.846	
		Mg II	7835	2798		
2322+396	B	Featureless				BL-Lac ?
2329+398	B	?	5010			Quasar
2335+392	B	Mg II	5751	2798	1.055	
		[O III]	6452	3133	1.059	$< z > = 1.059 \pm 0.003$
		[Ne V]	7062	3426	1.061	
2338+390	B	Mg II	5980	2798	0.82	
2344+429	B	C III	4866	1909	1.549	
		Mg II	7172	2798	1.563	$< z > = 1.556 \pm 0.01$
2349+410	B	C IV	4710	1549	2.041	
		C III	5825	1909	2.051	$< z > = 2.046 \pm 0.007$

Table 6. Quasar candidates with different spectroscopic identification

B3 name	Orig. ID	m_r	New ID	ref.
0000+394	N	17.5	STAR	
0003+380	N	17.0	SEYFERT	
0020+437	B	19.5	GAL/STAR	
0022+424	N	19.5	GAL	
0023+382	N	19.0	GAL	
0028+450	N	17.4	STAR	
0035+385A	B	18.5	GAL/STAR	
0045+395	N	16.0	BL-Lac	Djorgovski 95
0153+417	N	19.5	GAL	
0209+390	B	20.0	EF	
0217+395	N	18.5	STAR	
0218+402A	N	13.5	STAR	
0219+428A	B	16.0	BL-Lac	Veron 93
0228+392	N	13.5	STAR	
0709+409	N	20.0	GAL	
0739+397A	N	15.7	STAR	
0812+406	N	18.4	STAR	
0814+425	B	19.1	BL-Lac	Kühr 90
0820+431	N	19.5	GAL	
0841+403	N	19.5	GAL	
0902+414	N	17.5	GAL	
0902+416	N	19.5	STAR	
0904+399	N	17.5	GAL	
0936+405	N	18.5	GAL	
1012+389	N	20.0	EF	
1033+408	N	20.0	EF	
1128+455	N	18.5	GAL	
1245+396	B	17.7	STAR	
1258+395	N	18.5	EF	
1301+393	N	19.5	EF	
1317+389	B	19.7	EF	
1401+387	B	15.8	STAR	
1402+382	B	16.5	STAR	
1432+397B	N	18.5	GAL	
1457+388A	B	18.9	STAR	
2301+394B	N	20.0	STAR	
2301+398	N	19.5	STAR	
2301+430	N	16.0	STAR	
2311+396A	N	18.5	GAL/STAR/BL-Lac	
2322+396	B	17.8	BL-Lac?	
2330+435	N	15.4	STAR	
2336+381	N	17.5	STAR	
2355+398	B	18.0	STAR	

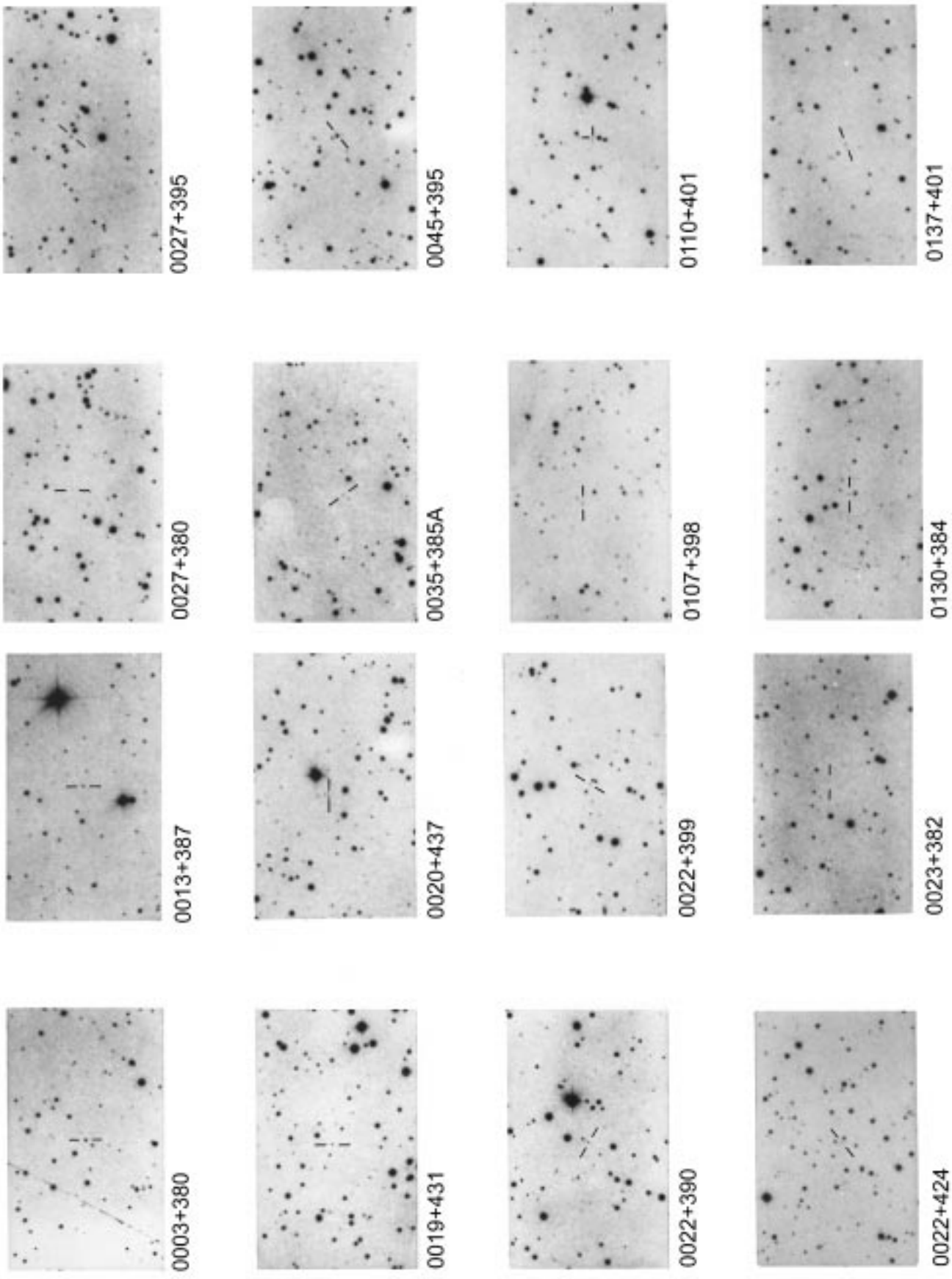

Fig. 5. Finding charts reproduced from the POSS−I for the objects listed in Table 5

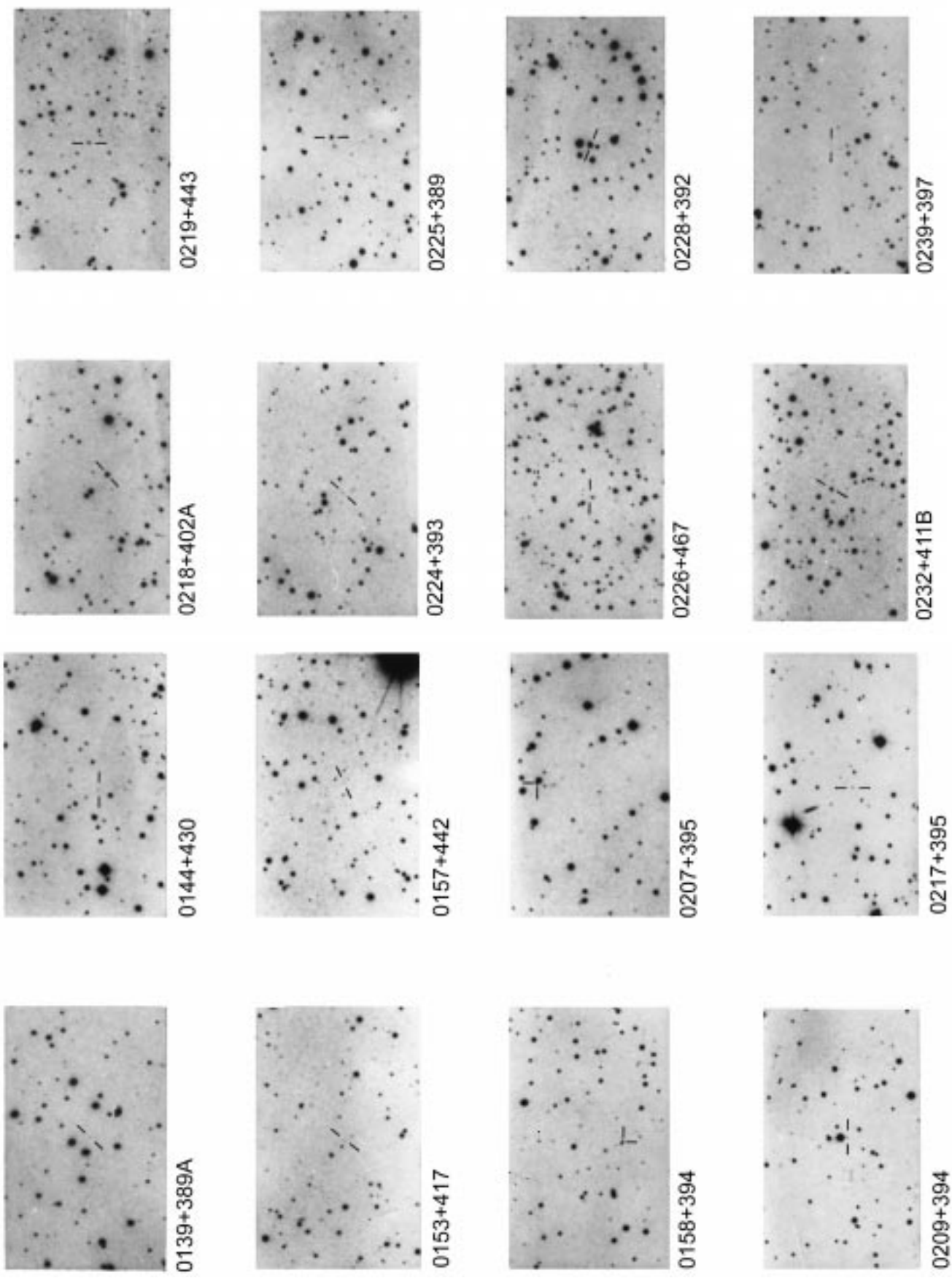

Fig. 5. continued

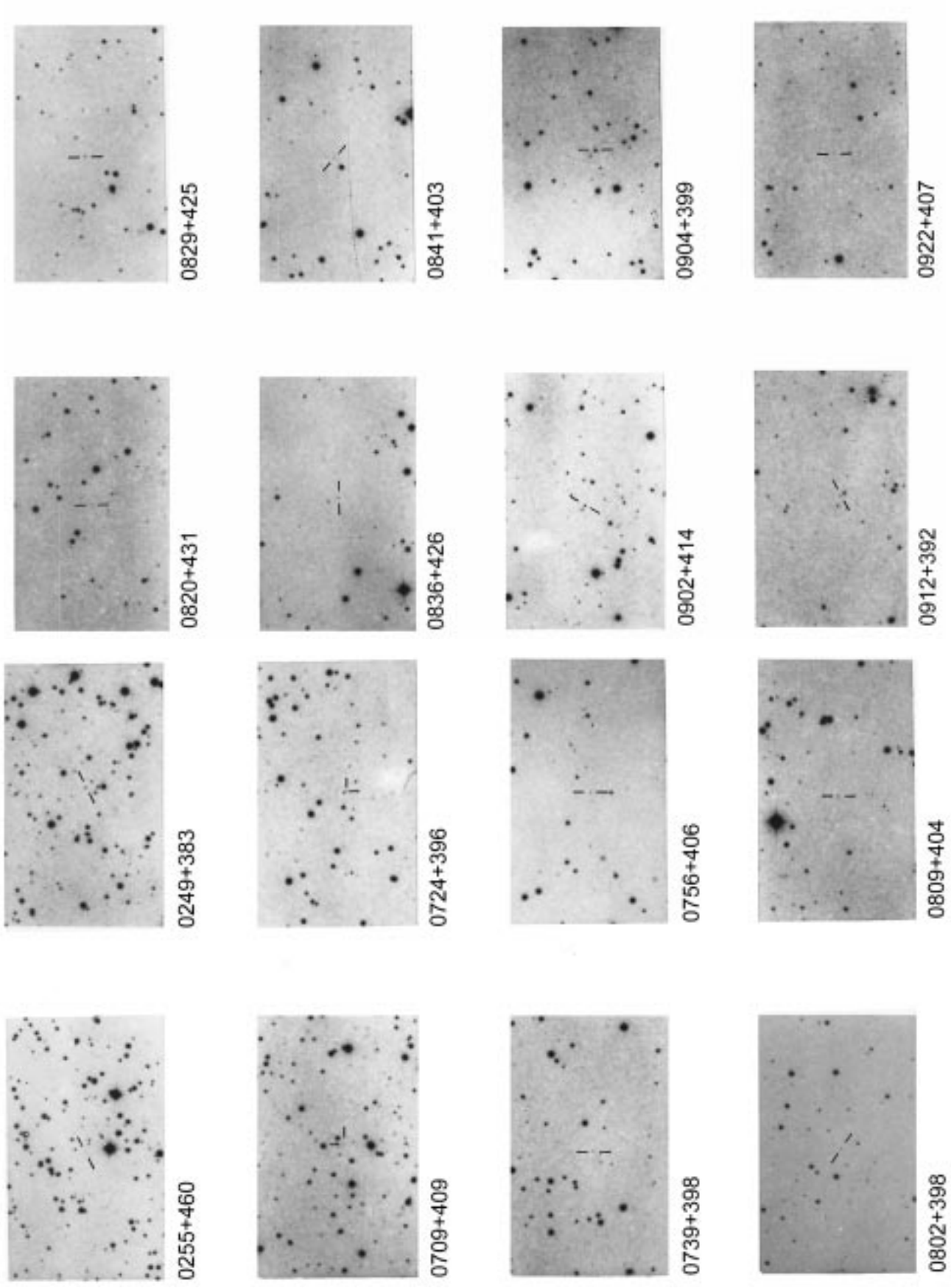

Fig. 5. continued

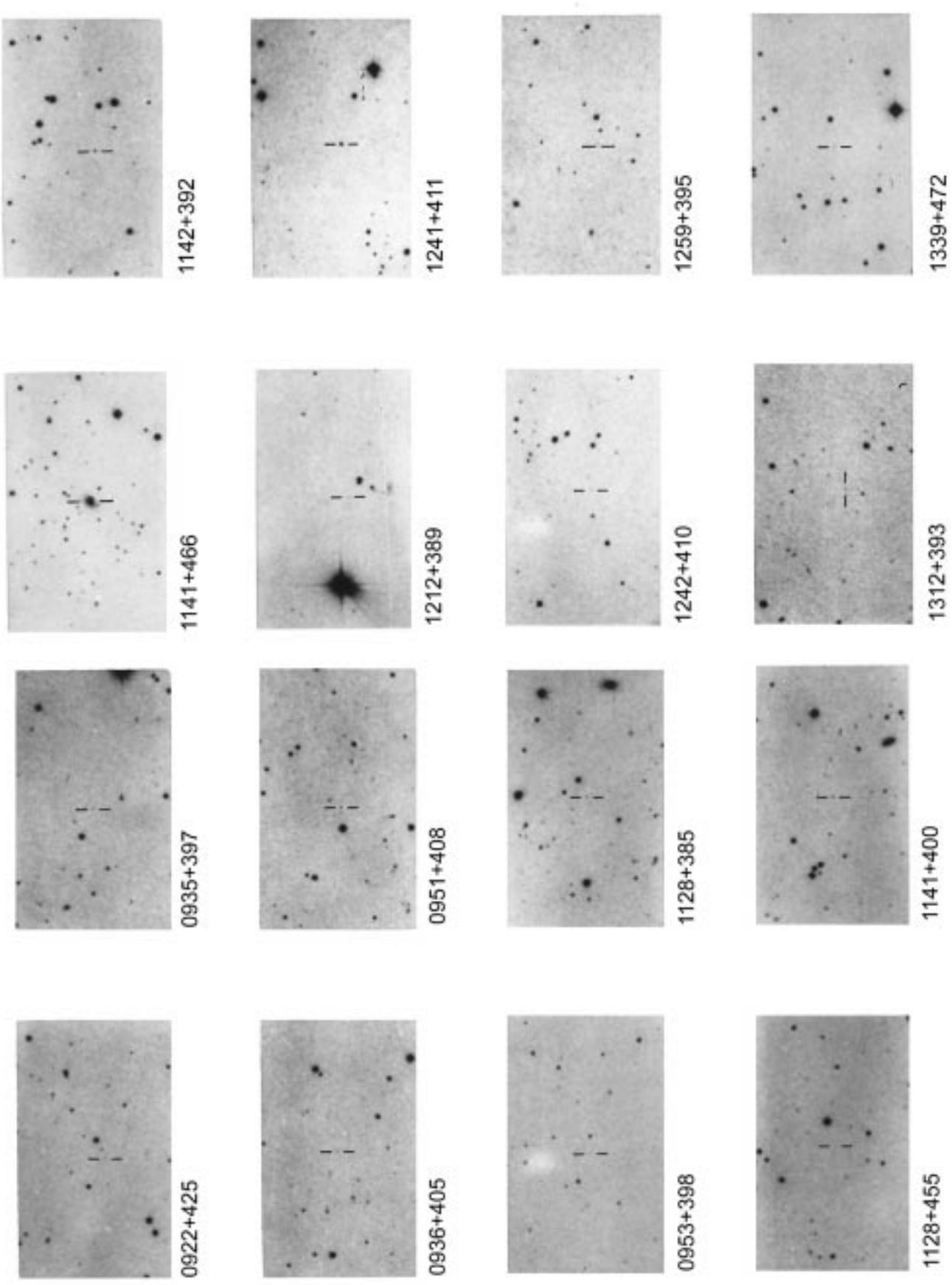

Fig. 5. continued

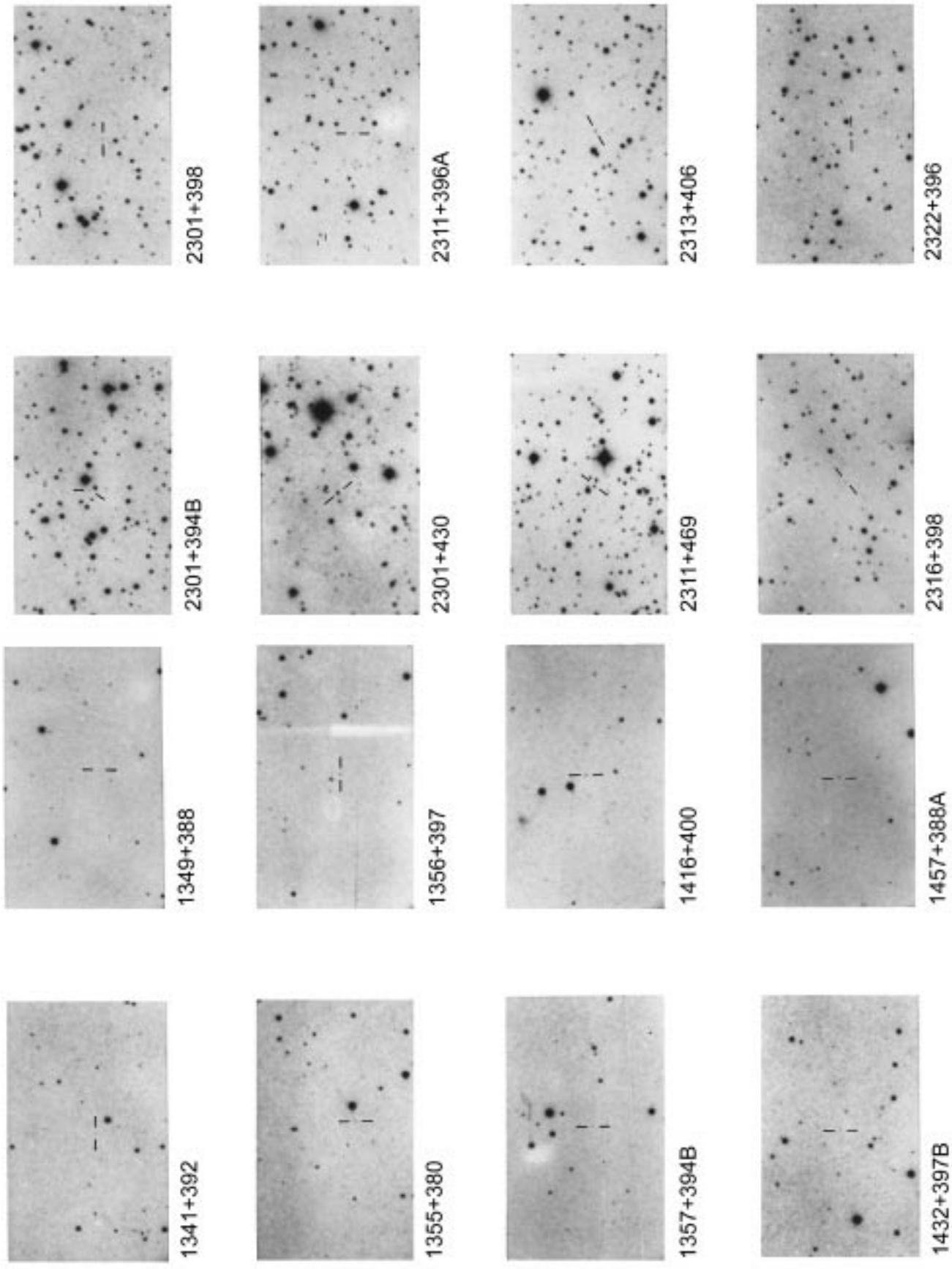

Fig. 5. continued

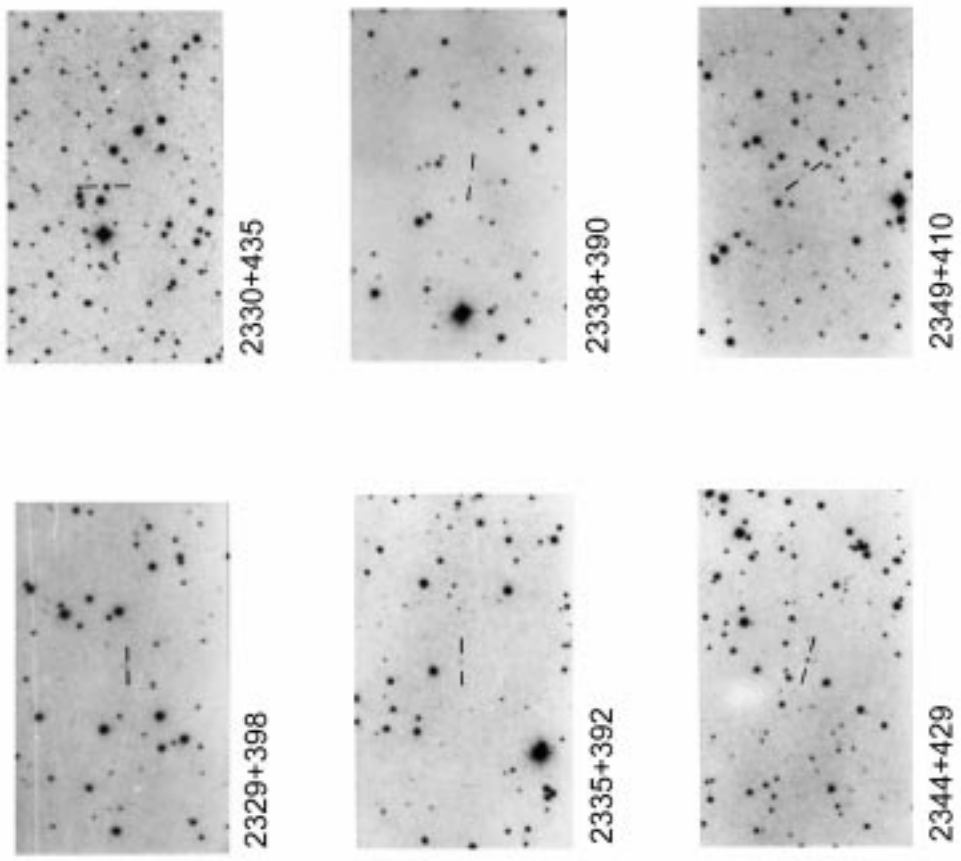

Fig. 5. continued